

# Verification and Validation of the Chapman Incompressible RANS Solver

Björn Regnström, Leif Broberg, Michal Orych, Magnus Östberg

Flowtech International AB, Gothenburg, Sweden

## Summary

This paper describes a verification exercise of a RANS code with a  $k$ - $\omega$  Baseline turbulence model. First a verification of the code by the use of manufactured solutions, where a 2D boundary layer look alike is used. The order of accuracy found is higher than 1 but lower than 2.

Then an uncertainty analysis of the manufactured case and a 2D backward facing step is performed. For the used grids the solver has some problems of predicting convergent values for local flow quantities, but behaves much better for integrated quantities.

Finally a validation against experimental data from the backwards facing step is done. In regions of uncomplicated flow the convergence is acceptable but the length of the recirculation region is under predicted by 11%.

## Introduction

Since the previous Lisbon workshop the discretization of the convective terms and the continuity equation have been replaced with a Fromm scheme. This apparently improved the prediction of ship wakes with bilge vortices, but no formal verification or validation of the code has not been done since the change.

## Numerical Method

To model the flow, the steady-state RANS equations together with Menter's  $k$ - $\omega$  Baseline (BSL) model (Menter, 1993) is used. The solid wall boundary condition for  $\omega$  is treated according to Hellsten and Laine (1997) which also allows for treatment of rough walls, but this feature was not used in the present investigation.

The equations are discretized with a finite volume

method. For the convective fluxes the approximate Riemann solver of Roe is used (Roe, 1981) (Kaurinkoski and Hellsten, 1998) (Vierendeels et al, 1999), while for the diffusive fluxes central differences around the cell face centers are used. Flux-correction with a min-mod limiter is used to increase the accuracy to second order in regions of smooth flow.

ADI is used to solve the equations. The tri-diagonal systems that are solved contains the first-order Roe convective terms and the second order diffusive terms, while the second-order flux corrections are used as an explicit defect correction. Each element in the tri-diagonal matrix is a  $5 \times 5$  matrix. For each sweep a local artificial time-step is calculated based on the CFL and von Neumann numbers in all directions except the implicit one. If it were not for the source terms in the turbulence equations the above described discretization will guarantee that  $k$  and  $\omega$  are kept positive. To maintain this in the presence of the source terms, the negative parts of the  $k$ - $\omega$  source terms are Newton-linearized and treated implicitly (Merci et.al. 2000). Strictly this does not guarantee positivity unless a time-step restriction is added, but in practice the artificial time-steps based on convection and diffusion are short enough that negative values of  $k$  and  $\omega$  do not occur.

## Boundary Conditions

Two layers of ghost cells are used around the boundaries. The variables in these cells are calculated at the same time as in the interior i.e. the values are updated within the ADI iteration.

For this exercise two different boundary conditions are used. The first one is Dirichlet boundary condition where a value of variable is specified on the boundary and extrapolated to the

ghost cells with second order accuracy.

The second is the Neumann boundary condition where a normal flux at the boundary is specified and used to linearly extrapolate to the ghost cells.

Since this treatment of the ghost points give to low order for the diffusive terms a special stencil is used for the diffusion along boundaries.

## Error Measures

For the interior the continuous  $L^1$  and  $L^2$  norms are used with the integrals approximated with sums over all cells

$$L^1 = \int_S |f| dS \approx \sum_i |f_i| S_i$$

$$L^2 = \left( \int_S |f|^2 dS \right)^{1/2} \approx \left( \sum_i |f_i|^2 S_i \right)^{1/2}$$

Due to the formulation of the discrete equations, the residuals are expressed as error per cell so in that case the terms in the sum are not multiplied by the cell volume.

## Uncertainty Estimation Procedure

An uncertainty estimation proposed by Eca, Hoekstra and Toxopeus (2005) is used. The following procedure were used:

- Determine the observed order of accuracy,  $p$ , from the available data.
- For  $0.95 \leq p < 2.05$ ,  $U_\phi$  is estimated with the Grid Convergence Index proposed and the standard deviation  $U_S$  of the fit:

$$U_\phi = 1.25 |\delta_{RE}| + U_S$$

The extrapolated value is taken as

$\phi_0 = \phi_1 + \delta_{RE}$  where  $\phi_1$  is the value from the finest grid.

- For  $0 < p < 0.95$ , the same error estimate is made but is then compared with the data range  $\Delta_M$  multiplied by the safety factor 1.25, so that  $U_\phi$  is obtained from:

$$U_\phi = \min(1.25 |\delta_{RE}| + U_S, \Delta_M)$$

If  $\Delta_M > 1.25 |\delta_{RE}| + U_S$  then  $\phi_0 = \phi_1$

- For  $p \geq 2.05$ ,  $U_\phi = 1.25 \Delta_M$ ,  
 $U_\phi = \min(1.25 |\delta_{RE}| + U_S, \Delta_M)$  where

$\delta_{RE}^*$  is calculated from a function with fixed  $p=2$  fitted to the data. The extrapolated value is  $\phi_0 = \phi_1 + \delta_{RE}^*$ .

- If monotonic convergence is not observed,  
 $U_\phi = 3 \Delta_M$  and  $\phi_0 = \phi_1$ .

## Test Case 1: Verification with Manufactured Solution

### Grids

The verification was done on a sequence of 4 Cartesian grids starting with 10x20 nodes and doubling the number of cells in both directions in each refinement so that the finest grid was 73x153 nodes.

### Boundary Conditions

In the table below,  $f_i$  is the  $i$ :th component of the manufactured solution.

| Left                                | Top                                 | Bottom                              | Right                                    |
|-------------------------------------|-------------------------------------|-------------------------------------|--|
| $u = f_u$                           | $u = f_u$                           | $u = 0$                             | $\frac{\partial u}{\partial n} = 0$      |
| $v = f_v$                           | $v = f_v$                           | $v = 0$                             | $\frac{\partial v}{\partial n} = 0$      |
| $\frac{\partial p}{\partial n} = 0$ | $\frac{\partial p}{\partial n} = 0$ | $\frac{\partial p}{\partial n} = 0$ | $\frac{\partial p}{\partial n} = 0$      |
| $k = f_k$                           | $k = f_k$                           | $k = 0$                             | $p = f_p$                                |
| $\omega = f_\omega$                 | $\omega = f_\omega$                 | $\omega = \omega_{wall}$            | $\frac{\partial k}{\partial n} = 0$      |
|                                     |                                     |                                     | $\frac{\partial \omega}{\partial n} = 0$ |

An improvement to this would be to use the normal derivatives of the manufactured solution  $\partial f_i / \partial n$  in the Neumann conditions.

### Results

The convergence rate  $p$  computed according to the uncertainty estimation procedure for the  $L^1$  and  $L^2$  norms of the solution minus the manufactured solution is given below.

|    | u    | v    | p    | k    | $\nu_t$ |
|----|------|------|------|------|---------|
| L1 | 1.93 | 1.38 | 2.00 | 2.00 | 2.00    |
| L2 | 1.98 | 1.69 | 1.69 | 1.62 | 2.00    |

Values equal to 2.00 indicate that  $p > 2.05$  and the fit has been re-computed with  $p = 2$ .

Verification of  $C_f$  yielded

| $C_F$                | $U(C_F)$             | $C_{Fmanu}$          |
|----------------------|----------------------|----------------------|
| $3.84 \cdot 10^{-6}$ | $0.43 \cdot 10^{-6}$ | $3.13 \cdot 10^{-6}$ |

## Test case 2: Validation with the Ercoftac Classic Database C-30 Backward Facing Step

### Grids

The same three grid sets supplied for the 2006 workshop were used with 101, 121, 141, 161, 181, 201 and 242 nodes in each directions. They will be referenced as g7, g6, g5, g4, g3, g2 and g1 respectively.

### Boundary Conditions

In the table below,  $g_i$  is the  $i$ :th component of the supplied inlet profile.

| Left  | Top  | Bottom   | Right  |
|---|--|--|--|
| $u = g_u$<br>$v = g_v$<br>$\frac{\partial p}{\partial n} = 0$<br>$k = g_k$<br>$\omega = g_\omega$ | $u = 0$<br>$v = 0$<br>$\frac{\partial p}{\partial n} = 0$<br>$k = 0$<br>$\omega = \omega_{wall}$ | $u = \cdot$<br>$v = 0$<br>$\frac{\partial p}{\partial n} = 0$<br>$k = 0$<br>$\omega = \omega_{wall}$ | $\frac{\partial u}{\partial n} = 0$<br>$\frac{\partial n}{\partial n} = 0$<br>$p = 0$<br>$\frac{\partial k}{\partial n} = 0$<br>$\frac{\partial \omega}{\partial n} = 0$ |

| Integrated        | SetA   | SetB   | SetC   |
|-------------------|--------|--------|--------|
| $(C_F)_{bottom}$  | 0.0306 | 0.0321 | 0.0313 |
| $U(C_F)_{bottom}$ | 0.0138 | 0.0014 | 0.0140 |
| $(C_F)_{top}$     | 0.0478 | 0.0467 | 0.0478 |
| $U(C_F)_{top}$    | 0.0205 | 0.0042 | 0.0202 |
| $(C_P)_{bottom}$  | 0.1076 | 0.1021 | 0.1008 |
| $U(C_P)_{bottom}$ | 0.0117 | 0.0082 | 0.0089 |

| x=0, y=1.1 | SetA    | SetB    | SetC    |
|------------|---------|---------|---------|
| u          | 0.6793  | 0.6907  | 0.6900  |
| U(u)       | 0.0312  | 0.0098  | 0.1970  |
| v          | 0.0146  | 0.0140  | -0.0132 |
| U(v)       | 0.0180  | 0.0283  | 0.0951  |
| p          | -0.0985 | -0.0903 | -0.1054 |
| U(p)       | 0.0142  | 0.0113  | 0.0885  |
| $\nu_t$    | 0.00145 | 0.00149 | 0.00143 |
| $U(\nu_t)$ | 0.00022 | 0.00006 | 0.00115 |

| x=1, y=0.1 | SetA    | SetB    | SetC    |
|------------|---------|---------|---------|
| u          | -0.1085 | -0.1145 | -0.0996 |
| U(u)       | 0.0619  | 0.1207  | 0.0488  |
| v          | 0.0119  | 0.0088  | 0.0117  |
| U(v)       | 0.0043  | 0.0043  | 0.0055  |
| p          | -0.1091 | -0.1092 | -0.1004 |
| U(p)       | 0.0225  | 0.0122  | 0.0047  |
| $\nu_t$    | 0.00156 | 0.00179 | 0.00146 |
| $U(\nu_t)$ | 0.00181 | 0.00178 | 0.00156 |

### Results

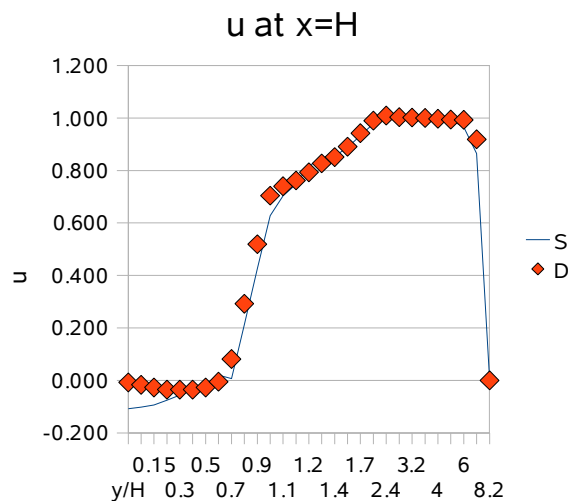
The results from the solution verification are given in the tables below

| x=4, y=0.1 | SetA     | SetB     | SetC     |
|------------|----------|----------|----------|
| u          | -0.0870  | -0.0829  | -0.0688  |
| U(u)       | 0.0505   | 0.0543   | 0.0673   |
| v          | -0.00801 | -0.00804 | -0.00891 |
| U(v)       | 0.00077  | 0.00072  | 0.00067  |
| p          | -0.0619  | -0.0545  | -0.0582  |
| U(p)       | 0.0085   | 0.0083   | 0.0154   |
| $v_t$      | 0.00605  | 0.00601  | 0.00592  |
| $U(v_t)$   | 0.000076 | 0.00015  | 0.00048  |

The results from the different grid sets are mostly consistent, even though SetC deviates for some data points. Looking at the uncertainties they are generally too large for successful validation (or falsification) of the computations.

With that said we proceed to look at the actual validation. The reattachment is predicted to close to the step,

| x-reattach | SetA  | SetB  | SetC  |
|------------|-------|-------|-------|
| S          | 5.516 | 5.480 | 5.669 |
| U(S)       | 0.587 | 0.108 | 0.577 |
| D          | 6.26  | 6.26  | 6.26  |



and this is the reason for the largest discrepancies between calculation and experiments, as exemplified by the u component of velocity at x=H in the plot above.

## Discussion

In most points the uncertainty in the computations is too large to allow validation. Even though the results compare relatively well to experiments in major parts of the domain, it would take a substantial reduction of the uncertainties to be able to positively consider the model validated or falsified. An investigation using finer grids, and possibly excluding some of the coarser grids in the current set, would be needed to resolve this issue.

To get a hint of whether the under prediction of the recirculation zone is a modeling error or a grid resolution problem, an EASM turbulence model will be applied to the same set of grids.

## References

- Hellsten, A., Laine, S. "Extensions of the k-w-SST turbulence model for flows over rough surfaces." AIAA AFM Conference Aug. 11-13, 1997, New Orleans, LA
- ITTC "Quality Manual: CFD General Uncertainty Analysis in CFD Examples for Resistance and Flow", 22nd ITTC, 1999
- Kaurinkoski, P., Hellsten, A. "FINFLO: the parallel multi-block flow solver" Report No A-17, Series A, Helsinki University of Technology, Laboratory of aerodynamics, 1998
- Menter, F.R. "Zonal Two Equation k- $\omega$  Turbulence Models for Aerodynamic Flows", 24th Fluid Dynamics Conference, Orlando, July 1993. AIAA paper 93-2906.
- Merci, B., Vierendeels, J., Reimslaugh, K., Dick, E. "Computational Treatment of Source Terms in Two-Equation Turbulence models", AIAA Journal Vol. 38, No. 11, Nov. 2000, pp 2085-2093.
- Roache, P.J., "Quantification of Uncertainty in Computational Fluid Dynamics", Annu. Rev. Fluid Mech. 29, 123-160, 1997.
- Roe, P.L., "Approximate Riemann Solvers, Parameter Vectors and Difference Schemes", J. Comp. Phys. 43, 310-341, 1981.
- Vierendeels, J., Reimslaugh, K., Dick, E. "A Multi-grid Semi-implicit Line-Method for

Viscous Incompressible Flow on High Aspect Ratio Grids", J. Comp. Phys. 154, 310-341, 1999.

Eca, L., Hoekstra, M., Toxopeus, S. "Calculation of the Flow around the KVLCC2M Tanker", CFD WORKSHOP TOKYO, 2005